JOURNAL OF GEOPHYSICAL RESEARCH, VOL. 104, NO. A3, PAGES 4467–4476, MARCH 1, 1999

Rapid enchancements of relativistic electrons deep in the magnetosphere during the May 15, 1997, magnetic storm

Xinlin Li,[1] D. N. Baker,[1] M. Teremin,[2] T. E. Cayton,[3] G. D. Reeves,[3] R. S. Selesnick,[4] J. B. Blake,[4] G. Lu,[5] S. G. Kanekal,[6] and H. J. Singer[7]

Abstract. Variations in 0.2–3.2 MeV electron flux in the magnetosphere during the May 15, 1997, magnetic storm (the largest magnetic storm of 1997) are examined. After over an order of magnitude initial decrease of the 0.2–3.2 MeV electron fluxes, the 0.2–0.8 MeV electron flux at $L < 4.5$ increased and surpassed the prestorm level in an hour. This increase was followed by increases of the more energetic 0.8–3.2 MeV electron fluxes. These energetic electron variations are examined utilizing data from the Solar, Anomalous, and Magnetospheric Particle Explorer (SAMPEX), the Global Positioning System (GPS) series of satellites, and the Los Alamos National Laboratory (LANL) sensors on board geosynchronous satellites. During the main phase of the storm, fluxes of >0.4-MeV electrons from SAMPEX decreased at $L > 4.5$ following the D_{st} drop but increased somewhat at $L < 4$. GPS satellite data also show that the electron flux decreased in the energy range 0.2–3.2 MeV for all L values above the minimum detectable L value of ~4.2 simultaneously with the decrease in D_{st}, which is consistent with an adiabatic process. However, the recovery of the electron flux was different at different energies, with an earlier recovery of the less energetic electrons and a later recovery of the more energetic electrons. The recovery of the electron fluxes started before the recovery of D_{st}, indicating that nonadiabatic processes were involved. The 0.2- to 0.8-MeV electrons appeared in the low-L region (4.2–4.5) at about the same time that the GOES 9 spacecraft measured a strong dipolarization of the Earth's stretched magnetic field. Outer zone electron fluxes continued to increase across a wide L range ($L = 3$–8) though the electron flux exhibited a strong spatial gradient, with the peak flux below $L = 4.2$ in the equatorial plane. These data are used to test the idea if radial transport from larger L can account for all of the increase in the flux in the heart of the outer zone electron radiation belt at $L = 4$–5. However, the radial gradient of the phase space density for a given first adiabatic invariant was estimated to be negative as a function of radial distance during the time that the electron flux was increasing. This estimate is somewhat uncertain because of rapid temporal variations and sparse data. However, if this estimate is correct, the usual theory of radial transport from larger radial distances cannot account for all of the increase in the electron flux. The analysis thus suggests that another process, such as local heating, which does not conserve μ, may be required to explain the subsequent enhancement of the more energetic (0.8- to 3.2-MeV) electrons but that additional data are required to answer this question definitely.

1. Introduction

Relativistic electrons in the magnetosphere have their largest variations during magnetic storms. The relativistic electron flux typically drops at the beginning of the main phase of a storm and starts to recover during the recovery phase of the storm and often exceeds prestorm levels after one or two days [*Paulikas and Blake*, 1979; *Baker et al*., 1990, 1994; *McIlwain*, 1996; *Li et al*., 1997a, b]. The initial drop of the electron flux is due, in part, to the adiabatic motion outward (conserving all three adiabatic invariants) of electrons as a consequence of the decrease of the magnetic field from the injection of the ring current [*Dessler and Karplus*, 1961; *McIlwain*, 1996]. We call this the D_{st} effect [*Li et al*., 1997b]. Since the loss of electrons often exceeds that which can be attributed to the D_{st} effect alone, additional losses such as precipitation into the atmosphere due to pitch angle scattering [*Kennel and Petschek*, 1966; *Lyons et al*., 1972] or drift into the magnetopause, when there is a strong compression of the dayside magnetosphere by the solar wind, often need to be invoked to explain adequately the observed loss of outer zone radiation belt electrons [*Li et al*., 1997b].

In this report we concentrate on the energization processes responsible for the recovery of the relativistic electron flux. These processes are less well understood. However, it is known that the recovery of the electron flux is also, in part, due to the

[1]Laboratory for Atmospheric and Space Physics, University of Colorado, Boulder.
[2]Space Sciences Laboratory, University of California, Berkeley.
[3]Los Alamos National Laboratory, Los Alamos, New Mexico.
[4]Space Sciences Department, The Aerospace Corporation.
[5]High-Altitude Observatory/National Center for Atmospheric Research, Boulder, Colorado.
[6]NASA/Goddard Space Flight Center, Greenbelt, Maryland.
[7]Space Environment Center/NOAA, Boulder, Colorado.

Paper number 1998JA900092.
0148-0227/99/1998JA900092$09.00

D_{st} effect. During the recovery phase of a magnetic storm the ring current decays and the equatorial magnetic field magnitude increases, leading to an adiabatic radial inward motion and energization of trapped radiation belt electrons. However, this D_{st} effect alone cannot explain the enhancement of electron fluxes above prestorm levels or the enhancement which occurs even before the recovery of the D_{st}. In reality, before D_{st} starts to recover, there will be fresh electrons injected into the magnetosphere, probably first at large L. As the ring current decays, these newly injected electrons will move farther inward and be adiabatically energized.

Transport of electrons from elsewhere in the magnetosphere or local heating of electrons are two alternatives available to explain such enhancements. The transport of electrons can be gradual in the form of radial diffusion because of magnetic and electric field fluctuations [*Schulz and Lanzerotti*, 1974; *Lyons and Schulz*, 1989] or rapid because of sudden impulses, which are associated with strong compressions of the magnetosphere by fast interplanetary shocks [*Li et al*., 1993, 1996a] or sudden pressure pulses [*Li et al*., 1998a, b]. Such compressions can quickly energize some of the preexisting electrons in the magnetosphere by moving them into stronger magnetic fields in a fraction of their drift periods. Alternatively, wave-particle interactions of electrons with, for instance, whistler waves may be invoked to explain the local heating of trapped radiation belt electrons [*Temerin et al*., 1994; *Horne and Thorne*, 1998; *Summers et al*., 1998]. While all of these mechanisms can occur, their relative importance for energization and transport of the outer belt electrons is not yet clear. In some individual cases, however, multiple spacecraft observations provide us a great opportunity to address this issue.

The magnetic storm of May 15, 1997, occurred because of a magnetic cloud, initiated by a coronal mass ejection, impinging on the Earth's magnetosphere. This event has been studied by *Baker et al*. [1998a], who suggest that some local acceleration processes, such as strong low-frequency magnetospheric waves, can quickly accelerate electrons to multi-MeV energies deep in the radiation belts on timescales of tens of minutes, as measured by POLAR and SAMPEX. Here we focus on detailed measurements from three GPS satellites of a sudden appearance of electrons in the energy range of 0.2–0.8 MeV in the magnetosphere at $L < 4.5$ and the subsequent enhancement of more energetic 0.8–3.2 MeV electrons even before the recovery of the D_{st}. These initial enhancements occurred on a timescale of tens of minutes and therefore are too fast to be explained by any adiabatic process (D_{st} effect) or radial diffusion. In addition to the short timescale, these enhanced fluxes also exhibit a strong spatial gradient with a peak below $L = 4.2$. With the help of upstream solar wind measurements from Wind, we confirm that these enhancements are not caused by any interplanetary shock or solar wind pressure pulse.

Here we argue using data from the May 15, 1997, magnetic storm that both fast radial transport and local heating may be important, with fast radial transport due to substorm injections or large electric fields that penetrate deep into the magnetosphere being the dominate process for lower energies (0.2–0.8 MeV). If this were generally the case during storms, it would imply that the outer radiation belt is generated by such processes rather than by radial diffusion since the observed radial diffusion during the quiet periods after a magnetic storm makes relatively small changes in overall character of the radiation belt.

2. Observations

Figure 1 shows various solar wind parameters measured by Wind during May 14–16, 1997, while Wind was moving from (193.5, −5.4, 17.7) to (185.6, −2.2, 16.8) R_E (Earth radius) in GSM coordinates. Figures 1a–1c show the solar wind velocity, density, and dynamic pressure (ρV^2) (courtesy of K. Ogilvie, 1998) [*Ogilvie et al*., 1995]; Figures 1d–1f show the three components (in GSM coordinates) and the magnitude of the interplanetary magnetic field (courtesy of R. Lepping, 1998) [*Lepping et al*., 1995]. The velocity, density, and hence the dynamic pressure increased sharply right after 0100 UT on May 15, marked by the vertical dashed line, when Wind was at (190.9, −3.9, 17.5) R_E. At this time the orientation and magnitude of the interplanetary magnetic field (IMF) also suddenly changed. This is identified as a strong forward shock and also the beginning of the influence of the magnetic cloud.

We now describe the response of the relativistic electrons in the magnetosphere to these solar wind conditions. Plate 1 shows the integral flux of >0.4 MeV electrons as a function of time during May 14–16, 1997, as measured by the proton/electron telescope (PET) instrument [*Cook et al*., 1993] on SAMPEX in a polar orbit with an altitude of 520 × 670 km and an inclination of 82° [*Baker et al*., 1993]. Only measurements taken during southern duskside (~ 17 magnetic local time (MLT)) passes are plotted in order to make a more consistent comparison in time. The temporal resolution is the orbital period (~ 96 min) and the L values are determined by mapping the field line using the International Geomagnetic Reference Field (IGRF) model 1990 extrapolated to the time of observation. No external fields are included in the calculation of L. The diurnal occurrence of the flux enhancement shown at $L \sim 2$ is due to contamination from every energetic protons (>4 MeV/nucleon) in the inner zone when the spacecraft crosses the South Atlantic anomaly (SAA) region. This orbital effect also produces a somewhat lesser variation of flux in the outer zone, where the flux is dominated by energetic electrons. In the outer zone, around 0900–1000 UT on May 15, an hour after sustained, strongly southward B_z, there was a decrease of the >0.4 MeV electrons at $L > 4.5$ but a slight increase at $L < 4$. Later, we see a continuous enhancement of the electron flux across a wide range of L (3–7) with the spatial peak moving to lower L (~ 4). Other instruments on SAMPEX, with higher energy thresholds (>1 MeV and 2–6 MeV), saw similar flux decreases but did not see the increase at $L < 4$ until about 1200 UT on May 15, as shown by [*Baker et al*., 1998a Figure 1]. Although the time resolution in Plate 1 is limited to the orbital period (~ 96 min), on average, it provides an overall picture of >0.4 MeV electrons in the magnetosphere during this period.

A more detailed view of the energetic electron flux variations can be seen by combining data from the GPS satellites, which are in circular orbits with a 12-hour orbital period at 4.2 R_E with an inclination of 55°. They pass close to the peak intensity region of the outer zone at low latitudes ($L = 4.2$) as well as larger L magnetic field lines at higher latitudes [*Drake et al*., 1993]. Plate 2 shows the counts per second in different energy ranges (0.2–0.4, 0.4–0.8, 0.8–1.6, 1.6–3.2 MeV) from three GPS satellites, each represented by a different color (NS24 = green, NS33 = red, NS39 = purple). Each satellite passes through a wide range of L values above a minimum L of ~ 4.2 four times during each orbit period (12 hours). By combining the three satellites one can get an almost continu-

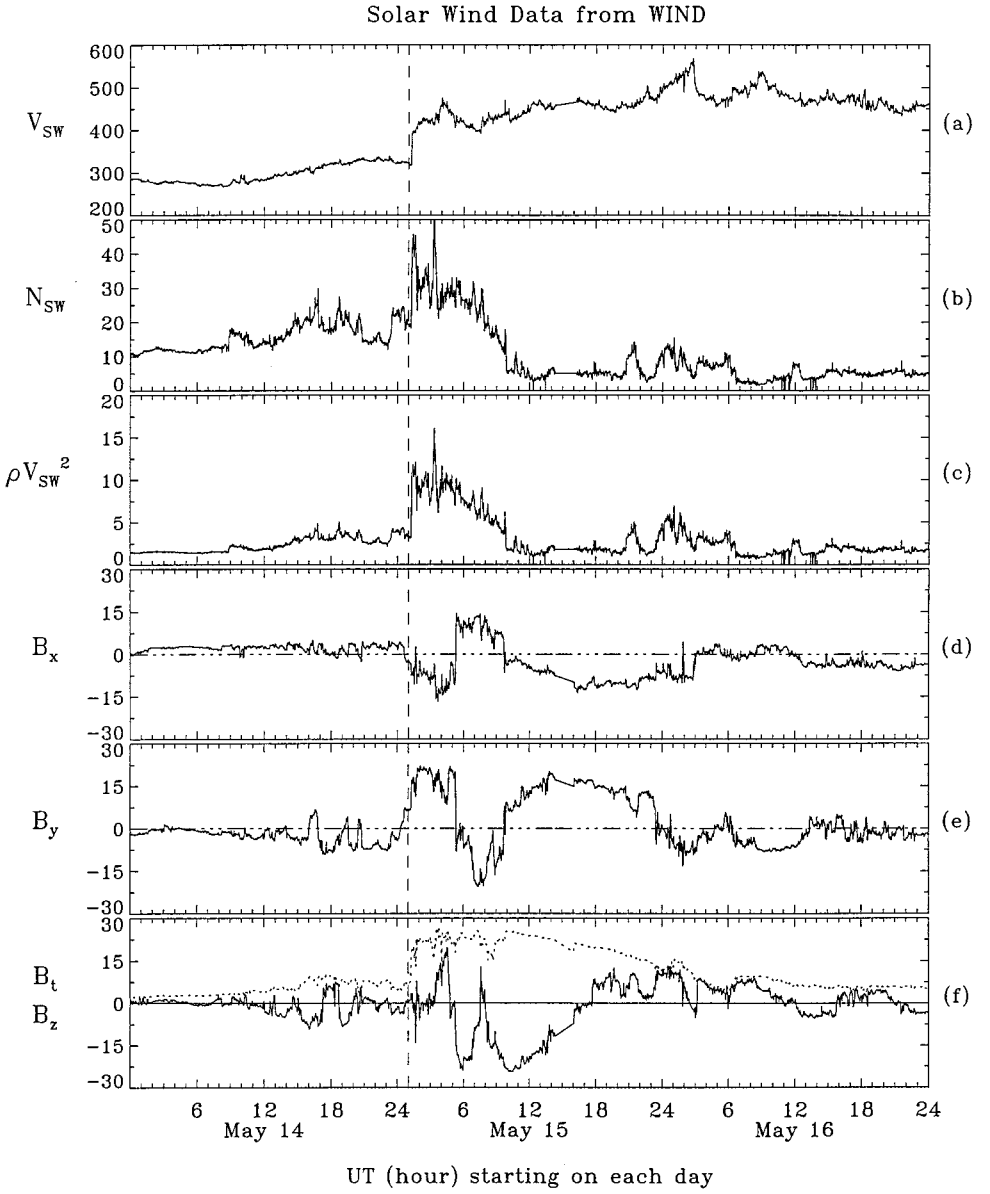

Figure 1. Various parameters plotted versus time for May 14–16, 1997: (a) solar wind velocity V_{sw}, (b) solar wind plasma density N_{sw}, and (c) solar wind dynamic pressure P_{sw} (every 90 s) (courtesy of K. Ogilvie, 1998), (d) B_x, (e) B_y, and (f) B_z components (in GSM coordinates), and magnitude (dotted line) of the interplanetary magnetic field (every 92 s) (courtesy of R. Lepping, 1998).

ous record of the energetic electron flux for $L > 4.2$. The L values used in presenting the GPS data are calculated from the interpolation formula by *Hilton* [1971] (also see *Schulz* [1996] for discussions of this L shell) using an updated IGRF model for the internal field and a quiet time Tsyganenko-89 model [*Tsyganenko*, 1989]. Each L diagram here is actually a plot of the count rate within 96-s bins when the GPS satellite is within 0.25 L of the nominal value. Thus the plot at $L = 4.5$ represents the data from the GPS satellites when they are between $L = 4.75$ and $L = 4.25$. The magnetic local time at 0000 UT on May 14 of the three GPS satellites is approximately 2154 for NS24 (green), 0815 for NS33 (red), and 1845 for NS39 (purple) and advances roughly 2 hours for each real hour. We have adjusted for the slightly different background count levels and effective geometric factors of the different GPS satellites and channels to produce a more uniform presentation. Also shown in Plate 2 is the 5-min resolution D_{st} index for May 15–16 (provisional D_{st} for May 14) calculated from 19 low- to mid-latitude ground magnetometer measurements. It should be noted that these three GPS satellites sample electrons at different MLT. A few hours in MLT make a significant difference in the observed flux changes at larger L. However, it is interesting to see that at low L (4.2–4.5) the three GPS satellites provide a continuous temporal record indicating that magnetic local time effects are small, as shown in Plate 2.

The electron fluxes in all energy ranges and all L values did not have any significant change until 0600 UT on May 15, when all fluxes decreased in association with the main phase of the storm, indicated by the D_{st} decrease. The temporal profile of the electrons resembles that of D_{st}; this aspect has been dis-

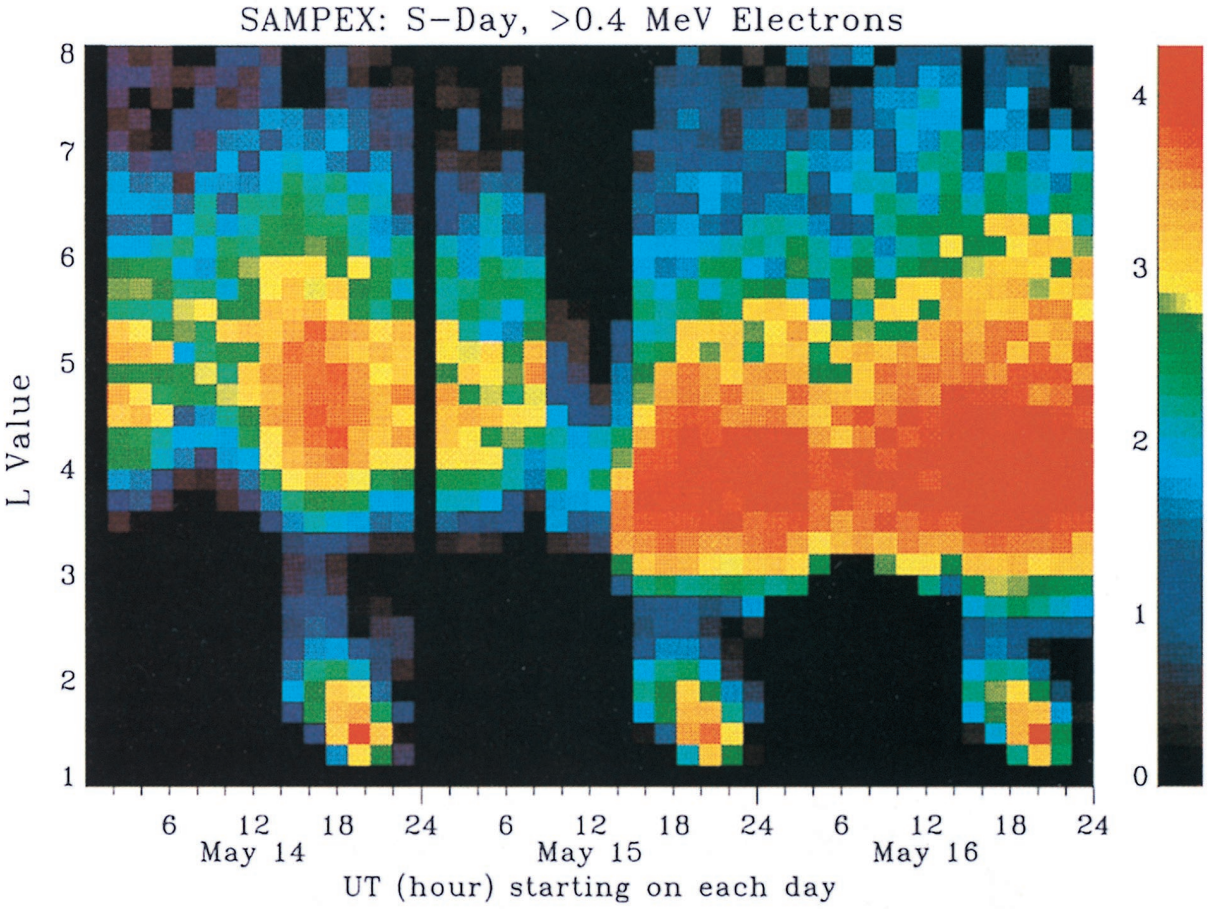

Plate 1. A color-coded representation of electron fluxes measured by the SAMPEX P1 channel (>0.4 MeV electrons and >4 MeV protons) during May 14–16, 1997. Only the southern dayside (~ 17 magnetic local time (MLT)) passes are plotted in order to make a consistent comparison in time. The time for each column of pixels (covering the whole L shell) is about 20 min. However, the time between adjacent columns of pixels is one orbital period (~ 96 min). The data are binned in 0.2 L values, and the range $1 \leq L \leq 8$ is shown. Electrons dominate the count rate for $2 \leq L \leq 8$.

cussed extensively before (such as *Dessler and Karplus* [1961], *McIlwain* [1966, 1996], *Li et al*. [1997b], and *Kim and Chan* [1997]). The decrease of D_{st}, caused by the ring current enhancement, is a measure of the decrease of the magnetic field. To first order, trapped energetic electrons move out during a D_{st} decrease in order to conserve their third adiabatic invariant, which is the magnetic flux inside their drift orbit. Conservation of the first two adiabatic invariants then implies that the electron loses energy. If the electron phase space density at fixed first (μ) and second (J) adiabatic invariants is increasing with L and the electron distribution is steeply falling with energy, as it usually is, a fixed-energy detector will see a drop in the flux when the ring current is enhanced. As they move out, some electrons may get lost by pitch angle scattering or by drifting through the magnetopause [*Li et al*., 1997b].

However, the striking feature of this storm, as shown in Plate 2, is the enhancement of the electrons of different energies at lower L values on May 15, which can be seen by combining multispacecraft measurements. While D_{st} was still depressed, a rapid enhancement of 0.2- to 0.8-MeV (red) electrons (left diagrams) down to $L = 4.2$ and $L = 4.5$ occurred around 1000 UT on May 15, a rapid enhancement of 0.8- to 1.6 MeV- (green) electrons (top right diagram) occurred around 1200 UT, and, finally, another rapid enhancement of 1.6- to 3.2-MeV (purple) electrons (bottom right diagram) was clearly visible around 1400 UT. Had we had only spacecraft NS39 (purple) measurements, we would not have known that the electron flux started to increase until 1400 UT; had we had only spacecraft NS39 (purple) and NS24 (green), we would not have known that the electron flux started to increase until 1200 UT. However, the rapid enhancement of 0.2- to 0.8 MeV-electrons already occurred around 1000 UT.

Another important feature of Plate 2 is the strong spatial gradient of the enhanced electron flux with the peak located below the minimum L value (~ 4.2) of GPS spacecraft, which is indicated by the "/\" shape of flux as a function of time during each (color) satellite's passage through the magnetic equator where $L \approx 4.2$ (see Appendix A for detailed descriptions). Though we mostly interpret this feature as indicating a spatial gradient, it also could be due to a pitch angle flux peak at 90°. If the pitch angle distribution of the electrons is strongly peaked at 90° at the equator (pancake-like), the GPS satellites would also measure more flux at lower L values when the spacecraft are near the equator even if the radial distribution does not have a gradient in L. Measurements from the HIST instrument [*Blake et al*., 1995] on POLAR indeed show that the pitch angle distribution of the enhanced electrons on May 15, 1997, is more pancake-like initially and gradually becomes

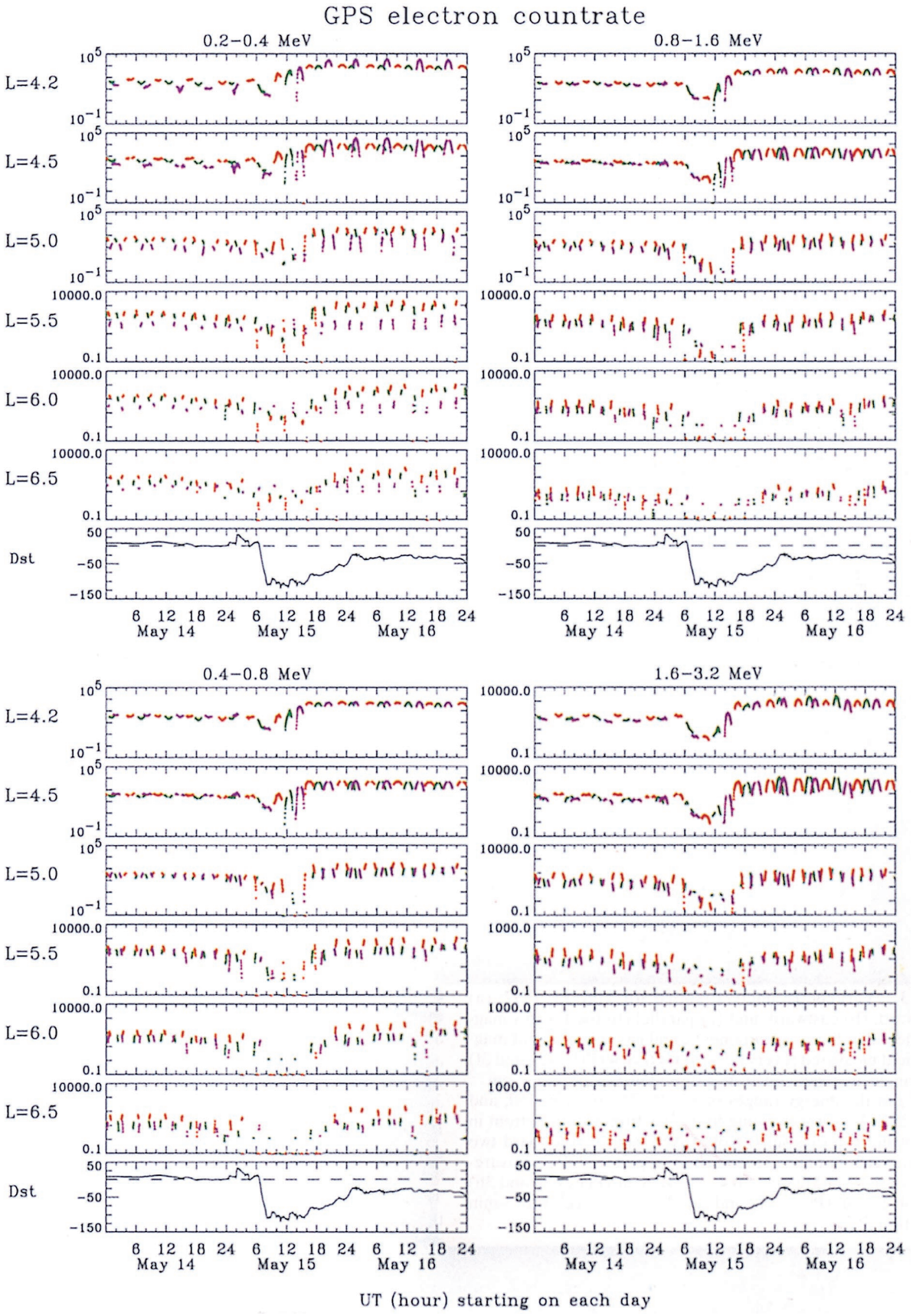

Plate 2. Count rate of electrons at various L values in various energy ranges from three GPS satellites, each represented by a different color (NS24 = green, NS33 = red, NS39 = purple), are plotted versus time for May 14–16, 1997. The provisional D_{st} for May 14 and high time resolution (every 5-min) D_{st} for May 15–16 are also plotted.

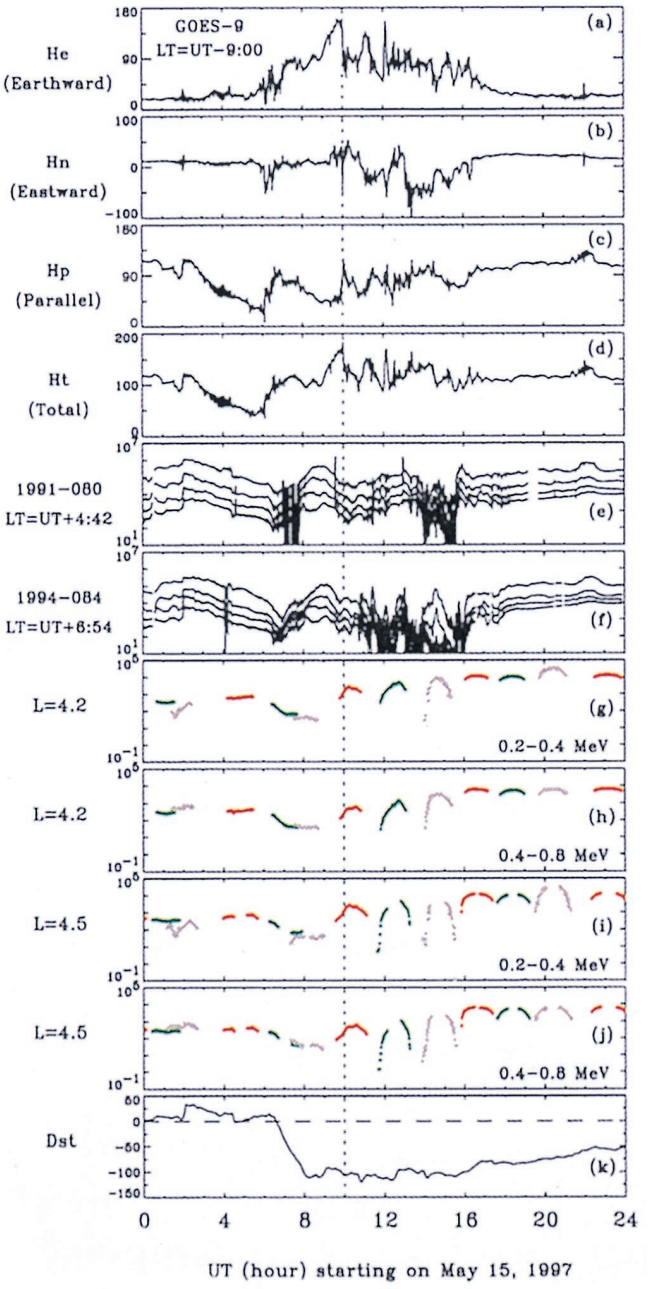

Plate 3. Various parameters plotted for May 15, 1997: (a) earthward, (b) eastward, and (c) parallel (to the Earth's magnetic field dipole axis) components, and (d) magnitude of magnetic field measured (every 0.5 s) at GOES 9; (Plates 3e and 3f) pitch angle averaged electron differential flux (s^{-1} sr^{-1} cm^{-2} keV^{-1}) in the energy ranges of 50–75, 75–105, 105–150, and 150–225 keV (corresponding four lines from top to bottom in each of the two diagrams) from LANL sensors on board two geostationary satellites (every 10 s); replot of GPS measurements of 0.2–0.4 MeV and 0.4–0.8 MeV at (Plates 3g and 3h) $L = 4.2$ and (Plates 3i and 3j) $L = 4.5$; (k) the 5-min resolution D_{st}.

more isotropic. For example, the ratio of the differential flux of 0.86 MeV electrons at a local pitch angle of 90° to the flux at 30° is 1.7 at $L = 4.2$–4.8 during the initial enhancement. About 8 hours later the ratio went back to <1.3. This is also a typical evolution of the pitch angle distribution for the relativistic electrons measured by the HIST instrument during more than 10 major magnetic storms ($D_{st} < -100$ nT). However, the ratio of GPS-measured electron fluxes at $L = 4.25$ to $L = 4.75$ is more than an order of magnitude. If the electrons have the same pitch angle distribution as measured by POLAR/HIST along the magnetic flux tube, the observed difference is too large to be accounted for by the pitch angle distribution and thus must be due to a spatial gradient. Note that before the storm the peak of the 0.2–1.6 MeV electron flux was between $L = 4.5$ and $L = 5$ and the peak of 1.6–3.2 MeV was between $L = 4.2$ and $L = 4.5$ (see Appendix A for detailed descriptions).

Plate 3 shows various magnetospheric parameters on May 15, 1997. Plates 3a–3d show the three components and the magnitude of the magnetic field as measured by GOES 9 at geostationary orbit. Plates 3e and 3f show the pitch angle averaged electron differential flux (s^{-1} sr^{-1} cm^{-2} keV^{-1}) in the energy ranges of 50–75, 75–105, 105–150, and 150–225 keV (the corresponding four lines from top to bottom in each of the two panels) from LANL sensors on board two geostationary satellites [*Belian et al.*, 1992]. Plates 3g–3j are replots of GPS measurements of 0.2- to 0.4-MeV and 0.4- to 0.8-MeV electrons at $L = 4.2$ and $L = 4.5$. Plate 3k is a replot of the 5-min resolution D_{st}.

Changes in solar wind conditions will result in responses from the magnetosphere. For example, the arrival of the forward shock, measured by Wind at (190.9, −3.9, 17.5) R_E in GSM coordinates at 0100 UT (marked by the vertical dashed line in Figure 1) was clearly registered at 0200 UT (marked by the vertical dashed line in Plate 3) by GOES 9 as jumps in H_p and H_t (indicating compression); by LANL sensors on two other geostationary satellites as abrupt increases in electron flux; and by ground magnetometer stations as a jump of D_{st} (compression). It was also visible at one GPS satellite, NS39 (purple), for 0.2–0.4 MeV electrons at $L = 4.2$ and $L = 4.5$, and less obviously for 0.4–0.8 MeV electrons, but still discernible.

The strong southward IMF, measured by Wind starting around 0500 UT (Figure 1f) while Wind was at (190.4, −0.7, 17.8) R_E in GSM coordinates, presumably arrived at Earth around 0600 UT, marking the beginning of the main phase of the storm. As the storm proceeded, substorm activity was also enhanced. The first dipolarization, indicated by a decrease of He (earthward) and an increase of Hp (parallel to the Earth's magnetic field dipole axis), was observed by GOES 9 at about 0600 UT (marked by the dash-dotted line). Energetic electron (50- to 225-keV) flux enhancements about half an hour after this time were recorded by LANL sensors at geostationary orbit (Plates 3e and 3f). The *AE* index calculated from 58 auroral zone stations was about 1700 nT at 0725 UT (not shown). Both LANL sensors were located in the afternoon sector when the first dipolarization occurred around 0600 UT. It would take more than half an hour for electrons with these energies to drift to the LANL sensors, assuming the injection associated with dipolarization occurred around local midnight. The main phase of the storm started soon after 0600 UT, and the total fluxes of relativistic electrons measured by GPS started to drop (D_{st} effect).

Later, the Earth's magnetic field on the nightside was stretched tailward from 0800 to 1000 UT as suggested by an increase of He and a decrease of H_p, as shown in Plates 3a and 3c. Then at 1000 UT, marked by the vertical dotted line, there was a sharp dipolarization, and at about the same time, 0.2- to 0.8-MeV electrons appeared deep in the magnetosphere as measured by GPS/NS33 (red) at $L = 4.2$ and $L = 4.5$ with

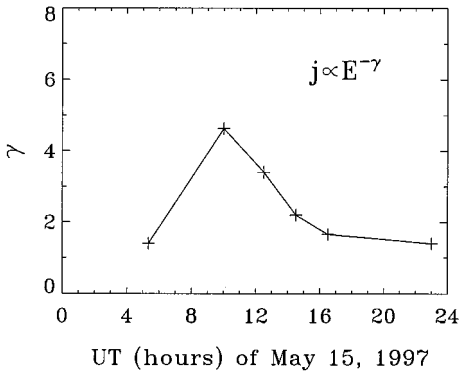

Figure 2. Spectral index plot for selected times. A power law was used to fit the 0.4- to 0.8-MeV and 0.8- to 1.6-MeV electron fluxes measured by GPS around $L = 4.2$.

the spatial peak below $L = 4.2$ (because of the "/\" shape at $L = 4.2$). We note from Figure 1 that there was no sudden pressure enhancement in the upstream solar wind around this time.

3. Discussion

We now discuss the possible causes for the electron enhancements.

3.1. Rapid Enhancement of 0.2–0.8 MeV Electrons

Lower-energy electrons are more easily affected by convective electric fields. During magnetic storms such electric fields change quickly and penetrate deep into the magnetosphere [*Rowland and Wygant*, 1998]. Fast changes in the convective electric field occur during substorms. Associated with the dipolarization as shown in Plate 3, there must be an inductive electric field according to the Faraday law, pointing westward and propagating earthward, which could have energized some of the preexisting electrons by quickly moving them into a stronger magnetic field [*Li et al*., 1998b]. This is similar to the effect of a solar wind shock or a solar wind pressure pulse induced electric field [*Li et al*., 1993, 1998a]. The enhanced energetic electron fluxes (50–225 keV) at geostationary orbit, peaked around 0900 UT as measured by LANL sensors (Plates 3e and 3f), could have been the source population for the electron enhancement by the inductive electric field of the dipolarization at 1000 UT in the lower L (stronger field) region. When the NS33 spacecraft (red) first measured the rapid enhancement of electrons in the 0.2- to 0.4- and 0.4- to 0.8-MeV channels at 1000 UT, this spacecraft (red) did not see any enhancement of >0.8-MeV electrons but actually saw a decrease of these electrons (see Plate 2, diagrams $L = 4.2$ for 0.8- to 1.6- and 1.6- to 3.2-MeV channels). At this time, this spacecraft (red) was located around 0600 MLT, consistent with the picture of substorm associated injections from the nightside. It is also consistent with the fact that substorms usually do not inject electrons with energies >400 keV into geosynchronous orbit [*Baker et al*., 1989; *Li et al*., 1996b] (this upper energy could be higher if injected into lower L).

FAST, which is in a polar orbit with an inclination of 83°, saw at about this time (0942–1045 UT) auroral activity down to at least 60° invariant latitude ($L = 4$). The observations indicate that the polar cap and auroral zone were greatly expanded and overlapped with the heart of the outer radiation belt at $L = 4$. Throughout the auroral zone, there were strong electric fields and wave turbulence, which may have been associated with the injection and acceleration of the relativistic electrons.

3.2 Subsequent Enhancements of 0.8–3.2 MeV Electrons

Let us use Plate 2 to examine the cause of the subsequent enhancements of the more energetic electrons (0.8–3.2 MeV) in the low L region (4.2–4.5) with a strong spatial gradient in the flux of these energy electrons peaking below $L = 4.2$. When the enhancement of 0.8- to 1.6-MeV electrons at $L = 4.2$ and $L = 4.5$ was first clearly measured around 1230 UT on May 15 (top right diagram, green; this spacecraft was located at 2230 MLT) and that of 1.6- to 3.2-MeV electrons was first clearly measured around 1430 UT at $L = 4.2$ and $L = 4.5$ (bottom right diagram, purple; this spacecraft was located at 2300 MLT), electrons of all energies (0.2–3.2 MeV) at larger L (>5) still had very low fluxes.

Using the GPS magnetic field model (since there was no direct magnetic field measurement available), we find that a 1-MeV electron at $L = 4.2$ would start with an initial energy of 0.36 MeV if coming from $L = 5.5$ while conserving μ. If the electron came from farther away, the required initial energy was smaller, and vice versa. Radial diffusion or radial transport proceeds by moving electrons from regions of higher phase space density to lower phase space density, and losses occur during the process of radial transport because of, for instance, pitch angle scattering. If the 1-MeV electron enhancement at $L = 4.2$ was due to only acceleration processes conserving μ, the phase space density for the same μ should be larger at $L = 5.5$ than at $L = 4.2$. However, assuming conservation of μ and that the pitch angle distribution at the equator is the same as measured by POLAR/HIST off the equator (see Appendix B), we estimate that the phase space density of 0.36-MeV electrons at the equator at $L = 5.5$ was more than 2 times smaller than the phase space density of 1-MeV electrons at the equator at $L = 4.2$. There are some uncertainties in the estimate, such as the lack of knowledge of the exact magnetic field and the pitch angle magnetic local time distribution of the electrons. However, this shortage of source electrons for given μ can be significant because, since only part of the source electrons at higher L (5.5) can be transported into lower L (4.2), some of the electrons are lost to the atmosphere because of pitch angle scattering while being transported inward. The above estimate suggests that energization processes that do not conserve μ may need to be invoked to account for the enhancement of 1-MeV electrons at $L = 4.2$.

3.3. Changes in the Energy Spectrum

Another interesting feature of the later enhancements of the more energetic electrons is the hardening of the energy spectrum as the flux recovered and surpassed the prestorm level. If we fit the GPS measurements of 0.4–0.8 MeV and 0.8–1.6 MeV with a power law, we obtain the power law index around $L = 4.2$ to be 4.63, 3.4, 2.2, 1.66, and 1.4 at 1000, 1230, 1430, 1630, and 2300 UT on May 15, as shown in Figure 2.

The softening of the energy spectrum at the beginning of the storm suggests that there was a greater loss of the more energetic electrons at the beginning of the storm, probably because more energetic electrons drift faster and experience more of the "effective" electric field associated with the ring current injections and also have a higher chance to hit the dayside magnetopause and get lost. This softening is also probably due

to the fact that less energetic electrons were continuously injected during the ring current enhancement.

The hardening of the spectrum later suggests that acceleration mechanisms which do not conserve μ during the recovery phase favor more energetic electrons in this region. Note that at 2300 UT on May 15, 1997, 0.8- to 3.2-MeV electron fluxes already surpassed the prestorm level by more than an order of magnitude, but D_{st} had not yet recovered and was still below −50 nT, as shown in Plate 2.

4. Summary and Conclusions

An analysis of multisatellite data has been performed for the outer radiation belt electron variations during the May 15, 1997, magnetic storm. SAMPEX, which provides a global picture of the radiation belt as a function of L near the foot of the field line, demonstrates the nearly simultaneous variation of the relativistic electrons over a large range of L values. The sudden enhancement of electrons in the energy range of 0.2–0.8 MeV deep in the magnetosphere at $L < 4.2$ and the subsequent enhancements of more energetic electrons (0.8–3.2 MeV) have been examined using three GPS satellite measurements. With better temporal and spatial resolution from multiple satellites we were able to view the temporal history of the electron enhancements.

An important question, perhaps the most important question, in radiation belt studies is whether radial transport is a sufficient explanation of the enhancements in the electron flux. We suggest that the sudden enhancement of the 0.2- to 0.8-MeV electrons down to below $L = 4.5$ can be due to injections of electrons from larger radial distances (while μ is conserved) associated with large-amplitude electric fields, but that a local heating process which does not conserve μ may have to be invoked to account for the subsequent enhancements of the more energetic (0.8- to 3.2-MeV) electrons peaking at $L < 4.5$.

The data also show the value of multisatellite measurements. Had we had only a single satellite measurement with a temporal resolution greater than 1 day [e.g., *Forbush et al*., 1961, 1962; *Owens and Frank*, 1968], we would have seen only a picture of the general pattern: the electron flux decreases during the main phase of the storm and recovers (often exceeds the prestorm level) starting during the recovery phase of the storm. Recently, we have investigated in detail using multisatellite data the outer radiation belt electron variations during magnetic storms of November 3–4, 1993, a solar wind high speed stream associated storm [*Li et al*., 1997b] on January 10–11, 1997, a magnetic cloud associated storm with a pressure pulse in the middle of the cloud [*Li et al*., 1998a; *Baker et al*., 1998b; M. K. Hudson et al., Simulation of relativistic electron flux increase on January 10–11, 1997, submitted to *Geophysical Research Letters*, 1998], and now, on May 15, 1997, another magnetic cloud associated storm but without a pressure pulse in the middle of the cloud. For a timescale greater than a day the electron flux variations during these storms show the same general pattern. However, they are different on finer timescales. For instance, the initial enhancement of 0.4- to 0.8-MeV electrons at $L = 4.2$–5 during the magnetic storm of November 3–4, 1993, closely followed the D_{st} recovery [*Li et al*., 1997b; *Kim and Chan*, 1997; *Freeman et al*., 1998], during the magnetic storm of January 10–11, 1997, the initial enhancement was well correlated with the arrival of a solar wind pressure pulse which also generated a D_{st} pulse, and now, during the magnetic storm of May 15, 1997, the initial enhancement did not seem to be associated with D_{st} recovery at all. For this May 15, 1997, magnetic storm, injections of 0.2- to 0.8-MeV electrons from larger radial distances and the local heating of more energetic electrons may be the dominant processes. These examples suggest that the dynamics of the energetic electrons in the magnetosphere are more complex than a single satellite can reveal. There are also other major magnetic storms during which the relativistic electrons may not follow the patterns mentioned above. There is still a great value in studying more individual events in detail before we can carry out a sensible statistical study to parameterize the variations of relativistic electrons during magnetic storms. Understanding the physical processes underlying the variation of the relativistic electrons in the magnetosphere is still a challenging task.

Appendix A: Spatial Location of the Flux Peak Inferred by Figure 3

The flux plotted at each nominal L value in Plate 2 includes an inbound pass (represented by the first stroke) from $L + 0.25 \Rightarrow L \Rightarrow L - 0.25$ and an outbound pass (the second stroke) from $L - 0.25 \Rightarrow L \Rightarrow L + 0.25$ (except $L = 4.25$, which covers from $L = 4.2$ to $L = 4.5$). When the spacecraft is close to its lowest L (low latitude), the inbound pass stroke and outbound pass stroke get close and even connect, producing a "$\vee$" or "$\wedge$" shape. A "$\vee$" indicates that the spacecraft measured fewer electrons (represented by "\" shape) as it went from $L + 0.25 \Rightarrow L \Rightarrow L - 0.25$ and then measured more electrons (represented by "/" shape) as it went from $L - 0.25 \Rightarrow L \Rightarrow L + 0.25$. So a "$\vee$" shape at a given L suggests that the peak is at a larger L. Likewise, a "$\wedge$" shape at a given L suggests the flux peak is at a lower L. This is how we know where the electron flux peaks and that the electron flux peak moved to a L smaller than the smallest L (~ 4.2) encountered by the GPS satellite after the enhancements.

Appendix B: Estimate of Phase Space Density at $L = 4.2$ and $L = 5.5$

The enhancement of 0.8- to 1.6-MeV electrons at $L = 4.2$ was first measured by NS24 (green) around 1230 UT on May 15 (top right panel of Plate 2), when NS24 was at the equator at 2300 MLT, where $B = 416$ nT (GPS model field). The earlier measurement of 0.2- to 0.8-MeV electrons was taken at $L = 5.5$ near 1115 UT on May 15, when NS24 (green) was off the equator at 2100 MLT, where $B = 569.7$ nT at the spacecraft position, and $B = 156.0$ nT at the equator ($L = 5.5$). If we fit the NS24 measurements of 0.2- to 0.4-MeV, 0.4- to 0.8-MeV, and 0.8- to 1.6-MeV electrons with a power law at 1115 UT on May 15, then

$$\int_{0.2}^{0.4} a_1 E^{n_1}\, dE = 4.125 \qquad \text{at} \quad L = 5.5 \tag{1}$$

$$\int_{0.4}^{0.8} a_1 E^{n_1}\, dE = 1.377 \qquad \text{at} \quad L = 5.5 \tag{2}$$

and at 1230 UT on May 15,

$$\int_{0.4}^{0.8} a_2 E^{n_2}\, dE = 718.89 \qquad \text{at} \quad L = 4.2 \tag{3}$$

$$\int_{0.8}^{1.6} a_2 E^{n_2}\, dE = 134.694 \qquad \text{at} \quad L = 4.2 \tag{4}$$

Solving (1)–(2) and (3)–(4) for a_1, n_1 and a_2, n_2, we have the differential fluxes (within a common constant factor):

$$j = 0.751E^{-2.6} \qquad L = 5.5 \text{ at } 1115 \text{ UT} \tag{5}$$

$$j = 236E^{-3.4} \qquad L = 4.2 \text{ at } 1230 \text{ UT} \tag{6}$$

So the omnidirectional differential flux of 1-MeV electrons at $L = 4.2$ at 1230 UT was 236.0, and the omnidirectional differential flux of 0.36-MeV electrons at $L = 5.5$ at the spacecraft location was 10.7. What should be the omnidirectional differential flux of 0.36-MeV electrons at $L = 5.5$ at the equator? Assuming that pitch angle α distribution at the spacecraft position is

$$j_d \propto \sin^{2n} \alpha \tag{7}$$

and assuming the same pitch angle distribution along the same magnetic flux tube, the flux at the equator for the corresponding equatorial pitch angle α_0 should be

$$j_{0d} = C_0 \sin^{2n} \alpha_0 \tag{8}$$

The Liouville theorem tells us that (assuming no loss of electrons)

$$j_d(\alpha) = j_{0d}(\alpha_0) \tag{9}$$

Conservation of the $\mu = p_\perp^2/2mB$ gives rise to

$$\sin^2 \alpha_0 = (B_0/B) \sin^2 \alpha \tag{10}$$

So the flux at the spacecraft position (equation (7)) can be written as

$$J_d = C_0(B_0/B)^n \sin^{2n} \alpha \tag{11}$$

The omnidirectional differential flux is simply an integration over pitch angle. So combining (8) and (11), we have that the ratio of the omnidirectional flux is

$$jo/j = (B/B_0)^n \tag{12}$$

To get n we use POLAR/HIST observations, which show that the ratio of flux at local 90° pitch angle to 30° is at most about a factor of 2. If we assume $j_d(90°)/j_s(30°) = 2$, we obatin $n = 0.5$. Then the ratio of the flux at the equator at $L = 5.5$ to the flux at the spacecraft position at $L = 5.5$ is

$$j_0/j = (B/B_0)^n = (569.7/156.0)^{0.5} = 1.911 \tag{13}$$

So the omnidirectional differential flux at the equator at $L = 5.5$ should be

$$j_0 = 1.991 \times j = 20.4477 \tag{14}$$

Now the corresponding phase space density of 0.36 MeV at the equator at $L = 5.5$ should be

$$f_p = j_0/p^2 = F_0 \times 10.742 \tag{15}$$

and the corresponding phase space density of 1 MeV at $L = 4.2$ should be

$$f_p = j_0/p^2 = F_0 \times 30.476 \tag{16}$$

where F_0 is a constant coming from $p^2 = F_0 \times \{(E + m_0c^2/m_0c^2)^2 - 1\}$. So the phase space density for a given μ at $L = 5.5$ is more than 2 times smaller than at $L = 4.2$. Note that the above estimation was based on some assumptions because of the available information on the pitch angle distribution. Also, note that this estimate is meant to be used only to compare the phase space density at two locations in a relative sense, so using only the relative values is sufficient.

Acknowledgments. The work at University of Colorado was supported by NASA grant NAG5-4896, NAG5-7112 and NSF grant ATM-9624390. Work at University of California at Berkeley was supported by NASA grant NAG5-3596. Work at Aerospace Corporation was supported by NASA contract NAS5-30368. Work at HAO/NCAR was supported by NASA ISTP Guest Investigator Program.

Janet G. Luhmann thanks Hee-Jeong and another referee for their assistance in evaluating this paper.

References

Baker, D. N., J. B. Blake, L. B. Callis, R. D. Belian, and T. E. Cayton, Relativistic electrons near geostationary orbit: Evidence for internal magnetospheric acceleration, *Geophys. Res. Lett*., *16*, 559, 1989.

Baker, D. N., R. L. McPherron, T. E. Cayton, and R. W. Klebesadel, Linear Prediction Filter analysis of relativistic electron properties at 6.6 R_E, *J. Geophys. Res*., *95*, 15,133, 1990.

Baker, D. N., G. M. Mason, O. Figueros, G. Colon, J. G. Watzin, and R. M. Aleman, An overview of the Solar Anomalous and Magnetospheric Particle Explorer (SAMPEX) mission, *IEEE Trans. Geosci. Remote Sens*., *31*, 531, 1993.

Baker, D. N., J. B. Blake, L. B. Callis, J. R. Cummings, D. Hovestadt, S. Kanekal, B. Blecker, R. A. Mewaldt, and R. D. Zwickl, Relativistic electron acceleration and decay time scales in the inner and outer radiation belts: SAMPEX, *Geophys. Res. Lett*., *21*, 409, 1994.

Baker, D. N., et al., A strong CME-related magnetic cloud interaction with the Earth's magnetosphere: ISTP observation of rapid relativistic electron acceleration on May 15, 1997, *Geophys. Res. Lett*., *25*, 2975, 1998a.

Baker, D. N., T. Pulkkinen, X. Li, S. Kanekal, J. B. Blake, R. S. Selesnick, M. G. Henderson, G. D. Reeves, H. E. Spence, and G. Rostoker, Coronal mass ejections, magnetic clouds, and relativistic magnetospheric electron events: ISTP, *J. Geophys. Res*., *103*, 17,279, 1998b.

Belian, R. D., G. R. Gisler, T. Cayton, and R. Christensen, High Z energetic particles at geosynchronous orbit during the great solar proton event of October 1989, *J. Geophys. Res*., *97*, 16,897, 1992.

Blake, J. B., et al., CEPPAD: Comprehensive energetic particle and pitch angle distribution experiment on POLAR, *Space Sci. Rev*., *71*, 531, 1995.

Cook, W. R., et al., PET: A proton/electron telescope for studies of magnetospheric, solar, and galactic particles, *IEEE Trans. Geosci. Remote Sens*., *31*, 565, 1993.

Dessler, A. J., and R. Karplus, Some effects of diamagnetic ring currents on Van Allen radiation, *J. Geophys. Res*., *66*, 2289, 1961.

Drake, D. M., T. E. Cayton, P. R. Higbie, D. K. McDaniels, R. C. Reedy, R. D. Belian, S. A. Walker, L. K. Cope, E. Noveroske, and C. L. Baca, Experimental evaluation of the BDD-I dosimeter for the Global Positioning System, *Nucl. Instrum. Methods Phys. Res*., *Sect. A*, *333*, 571, 1993.

Forbush, S. E., D. Venkatesan, and C. E. McIlwain, Intensity variations in the outer Van Allen radiation belt, *J. Geophys. Res*., *66*, 2275, 1961.

Forbush, S. E., G. Pizzella, and D. Venkatesan, The morphology and temporal variations of the Van Allen radiation belt, October 1959 to December 1960, *J. Geophys. Res*., *67*, 3651, 1962.

Freeman, J. W., T. P. O'Brien, A. A. Chan, and R. A. Wolf, Energetic electrons at geostationary orbit during the November 3–4, 1993 storm: Spatial/temporal morphology, characterization by a power law spectrum, and representation by an artificial neural network, *J. Geophys. Res*., *103*, 26,251, 1998.

Hilton, H. H., L parameter, a new approximation, *J. Geophys. Res*., *76*, 6952, 1971.

Horne, R. B., and R. M. Thorne, Potential waves for relativistic electron scattering and stochastic acceleration during magnetic storms, *Geophys. Res. Lett*., *25*, 3011, 1998.

Kennel, C., and H. Petschek, Limit on stably trapped particle fluxes, *J. Geophys. Res*., *71*, 1, 1966.

Kim, H.-J., and A. A. Chan, Fully adiabatic changes in storm-time relativistic electron fluxes, *J. Geophys. Res*., *102*, 22,107, 1997.

Lepping, R. P., et al., The WIND magnetic field investigation, The Global Geospace Mission, *Space Sci. Rev*., *71*, 207, 1995.

Li, X., I. Roth, M. Temerin, J. Wygant, M. K. Hudson, and J. B. Blake, Simulation of the prompt energization and transport of radiation particles during the March 23, 1991 SSC, *Geophys. Res. Lett*., *20*, 2423, 1993.

Li, X., M. K. Hudson, J. B. Blake, I. Roth, M. Temerin, and J. R. Wygant, Observation and simulation of the rapid formation of a new electron, *AIP Conf. Proc.*, *383*, 109, 1996a.

Li, X., D. N. Baker, M. Temerin, T. E. Cayton, E. G. D. Reeves, R. A. Christensen, and J. B. Blake, A source of outer radiation belt electrons: Substorm injections and further accelerations, paper presented at the Chapman Conference on the Earth's Magnetotail: New Perspectives, Inst. of Space and Astronaut. Sci., Kanazawa, Japan, Nov. 5–9, 1996b.

Li, X., D. N. Baker, M. Temerin, D. Larson, R. P. Lin, E. G. D. Reeves, M. D. Looper, S. G. Kanekal, and R. A. Mewaldt, Are energetic electrons in the solar wind the source of the outer radiation belt?, *Geophys. Res. Lett*., *24*, 923, 1997a.

Li, X., D. N. Baker, M. Temerin, T. E. Cayton, G. D. Reeves, R. A. Christensen, J. B. Blake, M. D. Looper, R. Nakamura, and S. G. Kanekal, Multisatellite observations of the outer zone electron variation during the November 3–4, 1993, magnetic storm, *J. Geophys. Res*., *102*, 14,123, 1997b.

Li, X., D. N. Baker, M. Temerin, T. E. Cayton, G. D. Reeves, T. Araki, H. Singer, D. Larson, R. P. Lin, and S. G. Kanekal, Energetic electron injections into the inner magnetosphere during the Jan. 10–11, 1997 magnetic storm, *Geophys. Res. Lett*., *25*, 2561, 1998a.

Li, X., D. N. Baker, M. Temerin, G. D. Reeves, and R. D. Belian, Simulation of dispersionless injections and drift echoes of energetic electrons associated with substorms, *Geophys. Res. Lett*., *25*, 3759, 1998b.

Lyons, L. R., and M. Schulz, Access of energetic particles to storm time ring current through enhanced radial "diffusion," *J. Geophys. Res*., *94*, 5491, 1989.

Lyons, L. R., and R. M. Thorne, Parasitic pitch angle diffusion of radiation belt particles by ion cyclotron waves, *J. Geophys. Res*., *77*, 5608, 1972.

Lyons, L. R., R. M. Thorne, and C. F. Kennel, Pitch-angle diffusion of radiation belt electrons within the plasmasphere, *J. Geophys. Res*., *77*, 3455, 1972.

McIlwain, C. E., Ring current effects on trapped particles, *J. Geophys. Res*., *71*, 3623, 1966.

McIlwain, C. E., Processes acting upon outer zone electrons, in *Radiation Belts: Models and Standards*, *Geophys. Monogr. Ser*., vol. 97, edited by J. F. Lemaire, D. Heynderickx, and D. N. Baker, pp. 15–26, AGU, Washington, D. C., 1996.

Ogilvie, K. W., et al., The WIND magnetic field investigation, The Global Geospace Mission, *Space Sci. Rev*., *71*, 55, 1995.

Owens, H. D., and L. A. Frank, Electron omnidirectional intensity contours in the Earth's outer radiation zone at the magnetic equator, *J. Geophys. Res*., *73*, 199, 1968.

Paulikas, G. A., and J. B. Blake, Effects of the solar wind on magnetospheric dynamics: Energetic electrons at the synchronous orbit, in *Quantitative Modeling of Magnetospheric Processes*, *Geophys. Monogr. Ser*., vol. 21, edited by W. P. Olsen, pp. 180–202, AGU, Washington, D. C., 1979.

Rowland, D., and J. R. Wygant, Dependence of the large-scale, inner magnetospheric electric field on geomagnetic activity, *J. Geophys. Res*., *103*, 14,959, 1998.

Schulz, M., Canonical coordinates for radiation-belt modeling, in *Radiation Belts: Models and Standards*, *Geophys. Monogr. Ser*., vol. 97, edited by J. F. Lemaire, D. Heynderickx, and D. N. Baker, pp. 153–160, AGU, Washington, D. C., 1996.

Schulz, M., and L. Lanzerotti, *Particle Diffusion in the Radiation Belts*, Springer-Verlag, New York, 1974.

Summers, D., R. M. Thorne, and F. Xiao, Relativistic theory of wave-particle resonant diffusion with application to electron acceleration in the magnetosphere, *J. Geophys. Res*., *103*, 20,487, 1998.

Temerin, M., I. Roth, M. K. Hudson, and J. R. Wygant, New paradigm for the transport and energization of radiation belt particles, *Eos Trans. Agu*, *75*(44), Fall Meet. Suppl., 538, 1994.

Tsyganenko, N. A., A magnetospheric magnetic field model with a warped tail current sheet, *Planet. Space Sci*., *37*, 5, 1989.

D. N. Baker and Xinlin Li, LASP/University of Colorado, 1234 Innovation Drive, Boulder, CO 80303-7814. (lix@kitron.colorado.edu)

J. B. Blake and R. S. Selesnick, Department of Space Sciences, Aerospace Corporation, Los Angeles, CA 90009-2957.

T. E. Cayton and E. G. D. Reeves, Los Alamos National Laboratory, Mail Stop D-436, Los Alamos, NM 87545.

S. G. Kanekal, NASA/GSFC, Code 690, Greenbelt, MD 20771.

G. Lu, HAO/NCAR, 3450 Mitchell Lane, Boulder, CO 80307.

H. J. Singer, NOAA R/E/SE, 325 Broadway, Boulder, CO 80303.

M. Temerin, Space Sciences Laboratory, University of California, Berkeley, CA 94720.

(Received May 20, 1998; revised September 18, 1998; accepted October 22, 1998.)